Vietnam Journal of Mechanics, Vol. 45, No. 4 (2023), pp. 287 – 295
DOI: https://doi.org/10.15625/0866-7136/18918

STUDY ON THE VELOCITY OF DROPLET AT STEADY STATE IN CONTRACTION MICROCHANNELS BY NUMERICAL SIMULATION

Thanh Tung Nguyen[1], Van Thanh Hoang[1,*], Duc Binh Luu[1], Ngoc Hai Tran[1], Minh Sang Tran[1], Le Hung Toan Do[1]

[1]*Department of Mechanical Engineering, The University of Danang - University of Science and Technology, 54 Nguyen Luong Bang Street, Danang City 550000, Vietnam*

[*]E-mail: hvthanh@dut.udn.vn

Received: 21 September 2023 / Revised: 27 October 2023 / Accepted: 11 November 2023
Published online: 05 December 2023

Abstract. The droplet-based microfluidic system is increasingly advancing and widely applied in various fields of analytical techniques and experiments. To optimize and advance this system, droplet dynamics is of utmost concern. The velocity of droplets is highly significant as it aids in precise droplet control and manipulation, ultimately leading to the optimization of device design and performance. This paper utilizes numerical simulations to explore the influence of flow characteristics, fluid properties, and geometric parameters of the contraction microchannel on the velocity of droplets while they are in a stable state. The findings indicate that the droplet velocity is influenced by factors such as viscosity ratio (λ), capillary number (Ca), and contraction ratio (C).

Keywords: droplet dynamics, droplet-based microfluidic, contraction microchannel, numerical simulation, velocity of droplets.

1. INTRODUCTION

The droplet-based microfluidic system has evolved into advanced technology, making significant contributions to the development of novel experimental methods. With remarkable advantages such as high speed, low sample and reagent consumption, ease of operation, and precise control, it has led to cost savings and time efficiency. Consequently, microfluidic systems have found diverse applications in fields such as biomedicine and chemistry [1].

In recent years, extensive research has been conducted on the dynamics of liquid droplets. For instance, Christafakis and Tsangaris [2] investigated the impact of Capillary number (Ca), Reynolds number (Re), Weber number (We), and viscosity ratio (λ) on the dynamics of liquid droplets in contraction microchannel systems. Similarly, Harvie and colleagues [3–5] explored the dynamics of droplets in contraction channels, focusing on the influence of Ca, Re, and λ. Most of these studies relied on two-dimensional numerical simulation methods, which, in cases involving non-circular channel geometries, exhibited limitations in accuracy, deviating from experimental results [6–8]. As a result, three-dimensional numerical simulations have become the preferred approach in numerous current research endeavors [9, 10]. Hoang et al. [11, 12] employed three-dimensional numerical simulation techniques to investigate droplet dynamics influenced by Ca and microchannel geometry in contraction microchannels.

One of the pivotal factors in dynamic analysis is the velocity of droplets within a contraction microchannel. Ling et al. [13] conducted a study assessing the influence of the height-to-velocity ratio of droplets in the Hele-Shaw system, while Thorben and colleagues [14] determined the excess velocity of Taylor droplets in square microchannels. Despite these investigations, a comprehensive evaluation of droplet velocity in contraction microchannels, considering the combined effects of three factors: viscosity ratio (λ), contraction ratio (C), perspective on droplet velocity influenced by the aforementioned factors, utilizing a three-dimensional numerical simulation method.

2. NUMERICAL SIMULATION

2.1. Geometric parameters of microchannels and flow characteristics

In Fig. 1, we present a contraction microchannels system with the geometric parameters under consideration. This system comprises two primary components: the larger microchannel and the contraction microchannel. The length and height of the larger microchannel are defined as 3D and 2D, respectively, while the contraction microchannel possesses dimensions of 15D in length and W in height, where D signifies the diameter of the liquid droplet. To mitigate the influence of sidewall deformations on the droplet's dynamics, a depth of 2.5D has been selected for the droplet [15–17]. These geometric parameters of the model have been verified and widely applied in the evaluation of droplet deformation and dynamics within contraction microchannels [11, 12].

In the microchannel, both liquid flow and droplets adhere to Newtonian fluid behavior, with laminar flow characteristics, and neglecting the influence of inertia. At the inlet of the larger microchannel, the flow has a constant velocity denoted as v_1, while within the contraction microchannel, we observe a characteristic average velocity denoted as v_2. The droplet's dynamics are governed by the dimensionless capillary number (Ca), which

is determined by the ratio of flow velocity (v), viscosity (μ_m), and surface tension (σ) between the droplet and the flow; expressed as: $Ca = \mu_m v/\sigma$. Ca_1 and Ca_2 correspond to velocities v_1 and v_2 in the larger microchannel and the contraction microchannel, respectively. The viscosity ratio (λ), characteristic of liquid properties, is defined as the ratio between the viscosity of the droplet and the viscosity of the flow; we define $\lambda = \mu_d/\mu_m$.

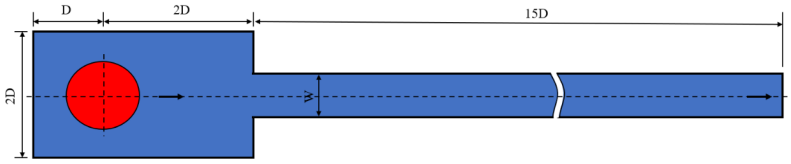

Fig. 1. Geometric parameters of microchannel

2.2. Simulation setup

During the simulation process, the height of the contraction microchannel was adjusted to represent different values of the contraction ratio ($C = D/W$) ranging from 1.25 to 2. Simultaneously, the values of σ and μ_d were varied to correspond to different values of Ca_2 and λ. The computational grid size was set to W/30 to ensure accuracy and uniformity across various C ratios, as demonstrated in previous studies [18]. The microchannel walls were identified as hydrophobic with a contact angle $\theta = 180^\circ$, and there was no slip. The outlet pressure remained constant and equal to zero. Due to the model's symmetry and computational efficiency, the simulation was conducted on one-quarter of the model.

The software ANSYS FLUENT is used for simulation. Certain computational techniques employed within this study encompass the PISO (Pressure-Implicit with Splitting of Operators) for coupling pressure and velocity, the PRESTO (Pressure Staggering Option) for interpolating pressure values, a Second-Order Upwind Scheme applied to conserve momentum equations, and the Geo-Reconstruct scheme, which plays a crucial role in interpolating interfaces [18].

The numerical model utilizes the Stokes flow equation, which is typically employed in situations characterized by low Reynolds numbers and high fluid viscosity:

$$\begin{aligned} \nabla u &= 0, \\ -\nabla p + \mu \nabla^2 u &= f, \end{aligned}$$

where u is the velocity vector, p is pressure, μ is dynamic viscosity, ∇u is the divergence of the velocity vector, $\nabla^2 u$ is the Laplacian of the velocity vector, f is the force vector.

The density and viscosity of the two-phase mixture in a computational cell are as follows:

$$\rho = \alpha_1\rho_1 + \alpha_2\rho_2,$$
$$\mu = \alpha_1\mu_1 + \alpha_2\mu_2,$$

where α_i, ρ_i, μ_i $(i = 1, 2)$ are the volume fraction, density, and viscosity of the first and second phases, respectively. The volume fraction of first phase can be obtained by solving continuity equation for volume fraction ($\alpha_1 + \alpha_2 = 1$).

3. RESULTS AND DISCUSSION

3.1. Steady-state droplet velocity in the microchannel

When a droplet moves within the constriction channel, its position is determined as follows: $Zd_n = (Zf_n + Zb_n)/2$. The parameters Zb and Zf at position t are illustrated in Fig. 2. At the position $Zd_i = (Zd_n - Zd_{n-1})/2$, the relative velocity of the droplet is calculated as $v_{di} = (Zd_n - Zd_{n-1}) / (t_n - t_{n-1})$. Additionally, we employ the ratio of droplet velocity v_d/v_2 to assess the velocity variation of the droplet at the normalized position Z_d/D.

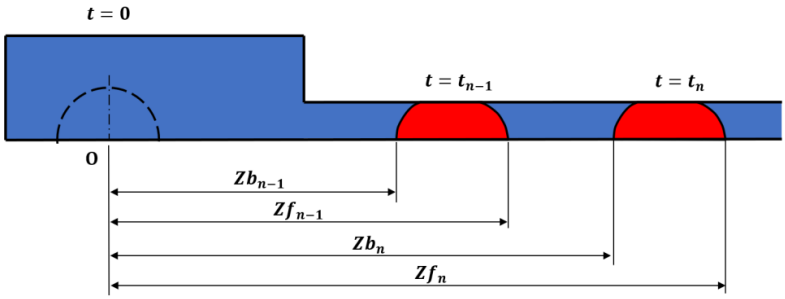

Fig. 2. Illustration of the dimensions that determine the velocity of droplet

As the flow transitions from v_1 in the larger microchannel to v_2 in the contraction microchannel, the droplet's velocity also undergoes changes. The variation in droplet velocity within the microchannel is depicted in Fig. 3. It can be observed that initially, the droplet's velocity increases rapidly, reaching its maximum velocity when the droplet has fully entered the contraction microchannel, after which it stabilizes. The droplet position reaching steady state is different for different viscosity values. When the viscosity is large, the droplet has larger deformation, which makes the stable position farther away [19]. Therefore, to ensure that the droplet's velocity is in a steady state, we examine the calculation of the droplet's velocity at the position $Z_d/D > 8$.

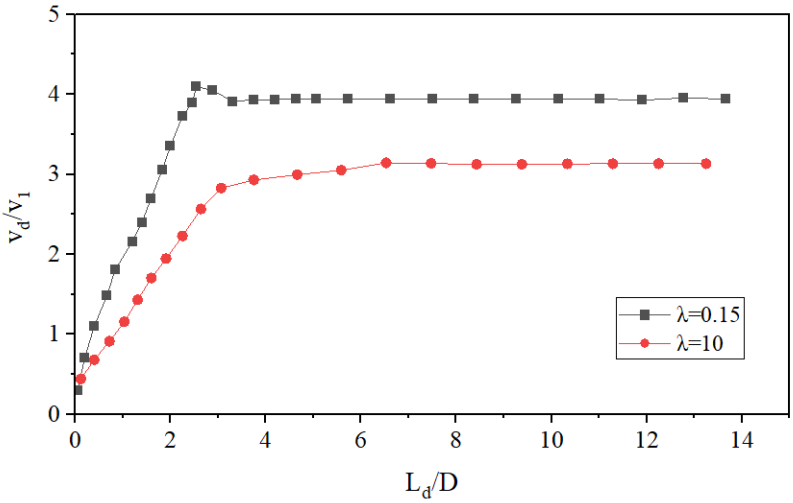

Fig. 3. The velocity ratio (v_d/v_1) of the droplet at different positions (L_d/D) in a contraction microchannel

3.2. Effect of viscosity ratio, capillary number, and contraction ratio on droplet steady velocity

In microfluidic systems, viscosity is a crucial factor influencing the fluid properties that significantly impact droplet dynamics. Fig. 4 presents the results illustrating the influence of viscosity ratio on the stable velocity ratio. The study involved varying the viscosity ratios across a range of 0.05 to 10, which are commonly employed values in microfluidic systems, while maintaining a constant contraction ratio of $C = 1.25$ and $Ca_2 = 0.1$. It can be observed that as λ increases, the droplet's velocity decreases. The droplet's velocity increases rapidly as λ decreases towards 0 and slightly decreases as λ surpasses a value greater than 1. Droplets move under the influence of viscous drag forces from the flow, and concurrently, these viscous drag forces deform the droplets, with droplets having λ greater than 1 undergoing more significant deformation compared to those with $\lambda < 1$ [19]. This results in the faster movement of less deformed droplets.

The Capillary number is directly proportional to the flow velocity, so it's possible to assess that an increase in Ca leads to an increase in the droplet's velocity, as demonstrated in Fig. 5. At a specific setting with $C = 1.25$ and $\lambda = 0.05$, the Ca_2 value was systematically varied within the range of 0.05 to 0.3 by altering the surface tension (σ) while keeping the flow velocity v_1 constant. Notably, as Ca_2 increased, the droplet velocity exhibited a rapid surge, elevating from an initial 1.2 to a peak of 1.82. With the increase in Ca, the surface tension of the droplet progressively loses its dominance, making the

droplet more susceptible to the influence of the flow, thereby increasing the droplet's velocity.

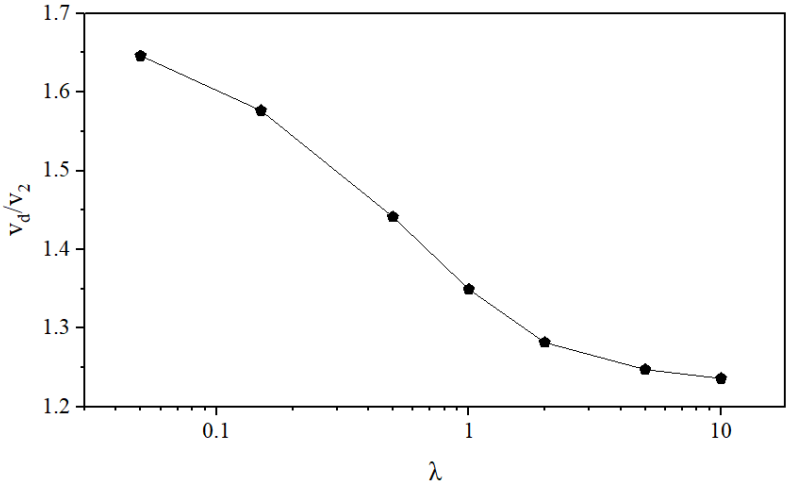

Fig. 4. Effect of viscosity ratio on droplet velocity ratio

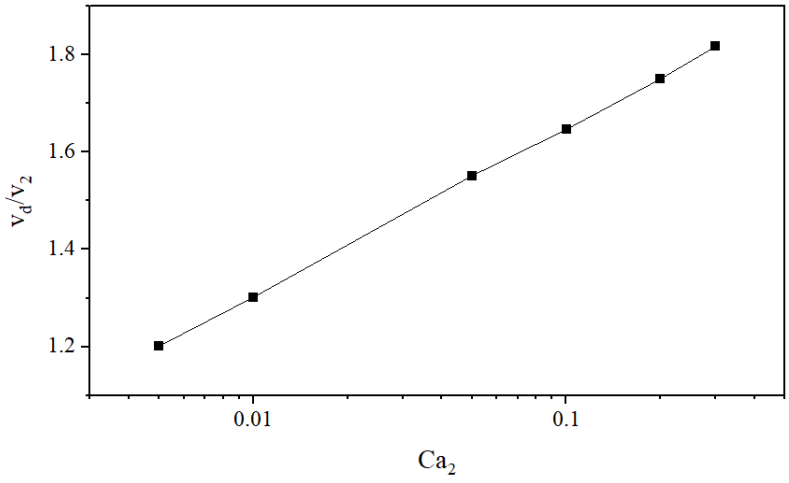

Fig. 5. Effect of capillary number on droplet velocity ratio

In addition to flow characteristics and fluid properties, the geometric parameters of the microchannel also influence the dynamics of the droplet. Evaluating the impact of microchannel geometry parameters aids in optimizing the design of the microchannel system. With the contraction ratio varying from 1.25 to 2 at $Ca_2 = 0.1$ and $\lambda = 0.05$, the droplet's velocity decreases from 1.646 to 1.59, as shown in Fig. 6. The droplet's velocity decreases due to the microchannel wall resistance, causing the droplet to experience

compression as the *C* increases. However, this change in velocity is relatively small when compared to the influence of λ and *Ca*.

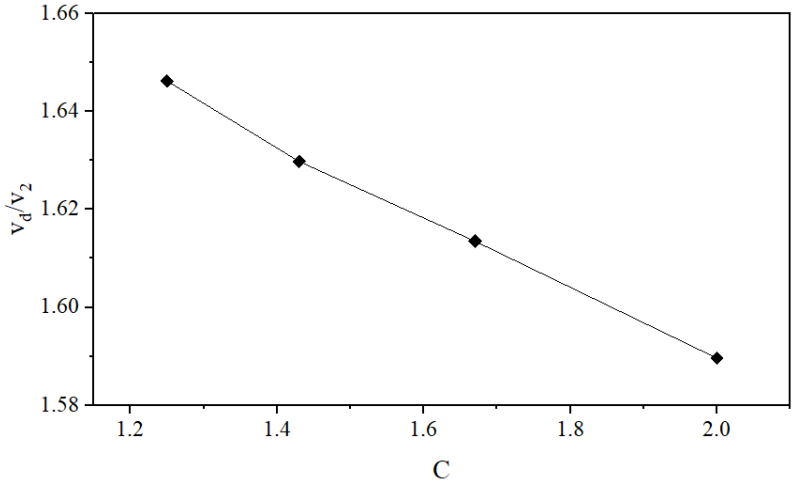

Fig. 6. Effect of contraction ratio on droplet velocity ratio

4. CONCLUSION

This study elucidates the influence of flow characteristics, fluid properties, and microchannel geometry parameters on the velocity of droplets within the contraction microchannel. Factors such as the capillary number (*Ca*), viscosity ratio (λ), and contraction ratio (*C*) play pivotal roles in the investigation of the droplet dynamics of the microfluidic system. Under the influence of the increasing flow velocity when transitioning from the larger microchannel to the contraction microchannel, the droplet's velocity initially rises and then reaches a stable state. The stable velocity of the droplet is significantly influenced by fluid properties and flow characteristics. The droplet velocity ratio increases as *Ca* increases or λ decreases. In contrast, the geometric parameters of the channel have a relatively minor effect, with an increase in *C* resulting in a reduction in the droplet velocity ratio compared to the flow.

DECLARATION OF COMPETING INTEREST

The authors declare that they have no known competing financial interests or personal relationships that could have appeared to influence the work reported in this paper.

ACKNOWLEDGEMENTS

This research is funded by Funds for Science and Technology Development of the University of Danang, under project number B2020-DN02-84. The authors would express

their acknowledgement to Professor Jang Min Park from School of Mechanical Engineering, Yeungnam University, the Republic of Korea for his support.

REFERENCES

[1] J. Castillo-León and W. E. Svendsen. *Lab-on-a-chip devices and micro-total analysis systems: A practical guide*. Springer International Publishing, (2015). https://doi.org/10.1007/978-3-319-08687-3.

[2] A. N. Christafakis and S. Tsangaris. Two-phase flows of droplets in contractions and double bends. *Engineering Applications of Computational Fluid Mechanics*, **2**, (2008), pp. 299–308. https://doi.org/10.1080/19942060.2008.11015230.

[3] D. J. E. Harvie, M. R. Davidson, J. J. Cooper-White, and M. Rudman. A parametric study of droplet deformation through a microfluidic contraction. *ANZIAM Journal*, **46**, (2005). https://doi.org/10.21914/anziamj.v46i0.953.

[4] D. J. E. Harvie, M. R. Davidson, J. J. Cooper-White, and M. Rudman. A parametric study of droplet deformation through a microfluidic contraction: Low viscosity Newtonian droplets. *Chemical Engineering Science*, **61**, (2006), pp. 5149–5158. https://doi.org/10.1016/j.ces.2006.03.011.

[5] D. J. E. Harvie, M. R. Davidson, J. J. Cooper-White, and M. Rudman. A parametric study of droplet deformation through a microfluidic contraction: Shear thinning liquids. *International Journal of Multiphase Flow*, **33**, (2007), pp. 545–556. https://doi.org/10.1016/j.ijmultiphaseflow.2006.12.002.

[6] I.-L. Ngo, T.-D. Dang, C. Byon, and S. W. Joo. A numerical study on the dynamics of droplet formation in a microfluidic double T-junction. *Biomicrofluidics*, **9**, (2015). https://doi.org/10.1063/1.4916228.

[7] D. J. E. Harvie, J. J. Cooper-White, and M. R. Davidson. Deformation of a viscoelastic droplet passing through a microfluidic contraction. *Journal of Non-Newtonian Fluid Mechanics*, **155**, (2008), pp. 67–79. https://doi.org/10.1016/j.jnnfm.2008.05.002.

[8] C. Galusinski and P. Vigneaux. On stability condition for bifluid flows with surface tension: Application to microfluidics. *Journal of Computational Physics*, **227**, (2008), pp. 6140–6164. https://doi.org/10.1016/j.jcp.2008.02.023.

[9] Z. Zhang, J. Xu, B. Hong, and X. Chen. The effects of 3D channel geometry on CTC passing pressure – towards deformability-based cancer cell separation. *Lab Chip*, **14**, (14), (2014), pp. 2576–2584. https://doi.org/10.1039/c4lc00301b.

[10] H. Liu and Y. Zhang. Modelling thermocapillary migration of a microfluidic droplet on a solid surface. *Journal of Computational Physics*, **280**, (2015), pp. 37–53. https://doi.org/10.1016/j.jcp.2014.09.015.

[11] V. T. Hoang, J. Lim, C. Byon, and J. M. Park. Three-dimensional simulation of droplet dynamics in planar contraction microchannel. *Chemical Engineering Science*, **176**, (2018), pp. 59–65. https://doi.org/10.1016/j.ces.2017.10.020.

[12] V. T. Hoang, V. D. Le, J. M. Park, and B.-T. Truong-Le. Effect of entry geometry on droplet dynamics in contraction microchannel. *International Journal of Multiphase Flow*, **167**, (2023). https://doi.org/10.1016/j.ijmultiphaseflow.2023.104543.

[13] Y. Ling, J.-M. Fullana, S. Popinet, and C. Josserand. Droplet migration in a hele–shaw cell: Effect of the lubrication film on the droplet dynamics. *Physics of Fluids*, **28**, (2016). https://doi.org/10.1063/1.4952398.

[14] T. Helmers, P. Kemper, J. Thöming, and U. Mießner. Modeling the excess velocity of low-viscous Taylor droplets in square microchannels. *Fluids*, **4**, (2019). https://doi.org/10.3390/fluids4030162.

[15] N. Ioannou, H. Liu, and Y. H. Zhang. Droplet dynamics in confinement. *Journal of Computational Science*, **17**, (2016), pp. 463–474. https://doi.org/10.1016/j.jocs.2016.03.009.

[16] S. Guido and M. Villone. Three-dimensional shape of a drop under simple shear flow. *Journal of Rheology*, **42**, (1998), pp. 395–415. https://doi.org/10.1122/1.550942.

[17] M. R. Kennedy, C. Pozrikidis, and R. Skalak. Motion and deformation of liquid drops, and the rheology of dilute emulsions in simple shear flow. *Computers & Fluids*, **23**, (1994), pp. 251–278. https://doi.org/10.1016/0045-7930(94)90040-x.

[18] X.-B. Li, F.-C. Li, J.-C. Yang, H. Kinoshita, M. Oishi, and M. Oshima. Study on the mechanism of droplet formation in T-junction microchannel. *Chemical Engineering Science*, **69**, (2012), pp. 340–351. https://doi.org/10.1016/j.ces.2011.10.048.

[19] V. T. Hoang and J. M. Park. A Taylor analogy model for droplet dynamics in planar extensional flow. *Chemical Engineering Science*, **204**, (2019), pp. 27–34. https://doi.org/10.1016/j.ces.2019.04.015.